# The Study of Jarosite Waste Used for Suspension Electrolysis in Aqueous NaOH Electrolyte

*Journal of The Electrochemical Society*, 2022 **169** 073506
1945-7111/2022/169(7)/073506/6/$40.00 © 2022 The Electrochemical Society ("ECS"). Published on behalf of ECS by IOP Publishing Limited

# The Study of Jarosite Waste Used for Suspension Electrolysis in Aqueous NaOH Electrolyte

**Bo Qin**[z] **and Geir Martin Haarberg**[*]

*Department of Materials Science and Engineering, Norwegian University of Science and Technology, NTNU, NO-7491 Trondheim, Norway*

Jarosite waste is normally generated from the purification process of zinc production. It contains many valuable elements such as zinc, lead, and especially iron. In the present study, jarosite waste was treated through thermal analysis and washing processes to concentrate hematite. An electrolysis process was used to reduce iron from the hematite in order to seek a new way to recycle the value of the resource. The electrochemical behavior of hematite in jarosite waste was studied by cyclic voltammetry at 100 °C in a 50 wt% NaOH aqueous solution. Constant cell voltage electrolysis was performed at 1.6 V by using electrolysis of a suspension of purified jarosite. Iron was found to deposit on a silver cathode during electrolysis. The sample was collected and analyzed by XRD.
 [DOI: 10.1149/1945-7111/ac7dca]

Manuscript submitted April 19, 2022; revised manuscript received June 13, 2022. Published July 11, 2022.

Jarosite is a natural mineral that can be found in acidic, sulfate-rich environments.[1] In metallurgical industry, jarosite is often generated as the major waste from the purification of zinc by hydrometallurgy processes.[2] It has the chemical formula $AFe_3(SO_4)_2(OH)_6$, where A is mainly $Na^+$, $K^+$, $NH^{4+}$ and $Pb^{2+}$ for zinc extraction industry. In order to remove three valent iron in the leaching solution of zinc, A ion is fed to react with $Fe^{3+}$ to form the residue under slightly acidic environments, where other impurities are also removed together by this way. Jarosite is insoluble in sulfuric acid and easy to collect. The reaction may be as follows:

$$3Fe_2(SO_4)_3 + 2(A)OH + 10H_2O = 2(A)Fe_3(SO_4)_2(OH)_6 + 5H_2SO_4 \quad [1]$$

Jarosite waste contains 25%−30% iron and 8%−12% sulfur, in addition, it also includes copper, nickel, silver, indium and other valuable metals,[3] which are mainly in the form of sulfates and oxides. Due to the large amount of the jarosite waste produced in zinc hydrometallurgy process,[4] its heaps not only occupy a lot of land resources, but also produce toxic elements and heavy metals that are discharged due to the change of the environment.[5] These hazardous substances, such as Pb are released and causing the soil to be polluted as well as water contamination. Because heavy metals cannot be biodegraded, the presence and the mobility of hazardous elements will lead to a serious environmental and social problem. Despite the presence of the issue for environmental damage, some metal elements within the waste have an intrinsic value to recovery. At present, some methods have been used to recover the valuable metals from jarosite waste. In these methods, pyrometallurgy [6,7] and hydrometallurgy [8,9] processes are commonly used, and there is also the joint process [10–12] for the treatment of jarosite waste. After recovery of the valuable metals, the residue containing iron oxide exhibits potential application as a resource for utilization in construction materials.[13–15] However, the technology still needs to be further improved to fulfill the utilization requirements as much as possible to ensure the stability of harmful components. Many works are focused on the recovery of valuable metals in jarosite waste, but for the large amount of iron there is lack of methods for recycling. Based on this, it is necessary to find a way to utilize this part of the resources.

Electrolysis of iron oxide at the low temperature is a novel technology. Iron can be produced by the direct electrochemical reduction of iron oxide that is suspended in a highly alkaline electrolyte containing 50 wt% NaOH.[16–18] During the electrolytic process, there is only oxygen evolution occurring at the anode, it means that $CO_2$ emissions is reduced significantly compared to the process by reduction of iron oxides by coal carbon at high temperature. As a matter of fact, not only iron-containing raw materials, such as iron ore or hematite, can be fed to this process to produce iron, but also some waste materials containing relatively high content of iron from process metallurgy as the source of iron oxide for electrolysis. The research [19] shows that hematite can be produced by thermal decomposition of jarosite, where the decomposition usually takes place at 500 °C−600 °C. Jarosite waste contains 25% − 30% iron, thus, it might also be as a source for the raw material of electrolysis. The aim of this study is to develop a potential process to recycle iron of jarosite waste without $CO_2$ emissions. The suitable process for metal recovery is expected to reduce the waste for environmental damage and make the most of this resource.

## Experimental

***Materials.***—The jarosite waste was provided by Boliden of Norway. The composition of the main metallic elements is analyzed by XRF and presented in Table I. Thermal analysis is beneficial for the study of jarosite. Firstly, thermal decomposition of the jarosite waste was carried out using TG-DSC under nitrogen atmosphere (10 ml $min^{-1}$). 11.774 mg of the sample was heated to 1000 °C with a heating rate of 10 °C $min^{-1}$. The decomposition products depend on the treatment temperature of the jarosite. After thermal decomposition, the specific temperature was chosen to treat the jarosite waste, and then the product was washed by two-step processing to enrich hematite.

The electrolyte was a 50 wt% NaOH aqueous solution, where sodium hydroxide (NaOH, Merck 99.0%) was used and dissolved in Milli-Q water. Silicone oil (Alfa Aesar) was placed in the beaker placed on a hotplate with magnetic stirring, and it served as heating bath for the lab-scale electrolytic cell. The temperature of the electrolyte was heated to 100 °C by the oil bath.

***Electrochemical apparatus.***—After thermal treatment, the electrochemical experiments were carried out in a container (Ø 100 mm, 160 mm height) made by polytetrafluoroethylene (PTFE). The lab-scale electrolytic cell is shown in Fig. 1a. Cyclic voltammetry was performed by using a three-electrode system. The cavity electrode was used as the working electrode for cyclic voltammetry studies. This electrode is suitable for electrochemical research in which materials are insoluble in the electrolyte.[20] The schematic of the cavity electrode is shown in Fig. 1b,[21] where its size is marked on the figure. A steel rod served as the current collector. The powder was put into the cavity during the CV experiments. After the tests, the cavity electrode was removed from the electrochemical cell, then the residual powder was cleaned for the next test with new powder.

*Electrochemical Society Member.
[z]E-mail: boqi@ntnu.no

**Table I. The composition of impurity elements in jarosite by XRF.**

| Element | Al | As | Ca | Cu | Fe | Mn | Pb | S | Sb | Si | Sn | Zn |
|---|---|---|---|---|---|---|---|---|---|---|---|---|
| Content % | 1.2 | 0.18 | 1 | 0.5 | 25 | 0.55 | 4.9 | 12.5 | 0.08 | 1.6 | 0.45 | 8.6 |

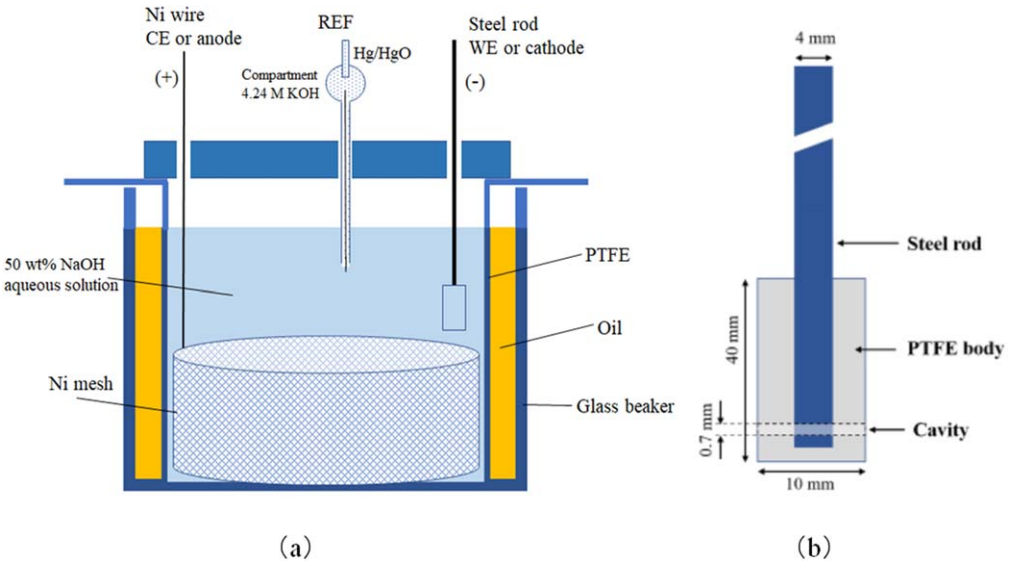


**Figure 1.** Schematic diagrams of the experimental set-ups for electrochemistry.

A nickel mesh served as the counter electrode, and it was made into the shape of a cylinder near the inside wall of the electrochemical cell and surrounding the cathode. Ni wire also served as the current collector. The reference electrode included three parts: a commercial single junction Hg/HgO electrode with 4.24 M KOH filling solution, a glass compartment containing 4.2 M KOH solution and a silver wire. The Hg/HgO electrode and silver wire were both immersed in the solution of the glass compartment. The other end of the silver wire was dipped into the electrolyte. The reference electrode was placed as close as possible to the working electrode.

After the study of cyclic voltammetry, a silver plate was used to take the place of the working electrode as the cathode. The nickel mesh was used as the anode. The electrolysis experiment was carried out in the cell, where the particles of the product obtained by thermal decomposition were suspended in the NaOH 50 wt% aqueous solution.

***Instrumentation.***—Thermogravimetric Analysis-differential scanning calorimetry (TG-DSC, NETZSCH) was used for heat analysis. The voltammetry studies were performed with an Autolab PGSTAT 30 computer controlled potentiostat. The product was collected and washed with distilled water, and then dried under vacuum for 2 h to prepare for examining by X-ray diffraction (XRD Bruker D8).

## Results and Discussion

***Thermal analysis.***—The thermal analysis of jarosite waste is shown in Fig. 2. This figure shows the thermogravimetry curve and the differential scanning calorimetry curve for jarosite waste. There are three steps of mass loss observed at 345 °C–440 °C, 578 °C–686 °C and 686 °C–766 °C, the mass losses being 7.2%, 7.5% and 4.8% respectively. From the corresponding curve of DSC, there are three endothermic peaks appeared in the curve. It means that there is the situation of solid-solid phase transition or release of gas. The first peak is near 440 °C, the second peak at 670 °C and the last one at 760 °C. As mentioned above, hematite can be obtained by thermal decomposition of jarosite at 500 °C − 600 °C, thus, the temperature

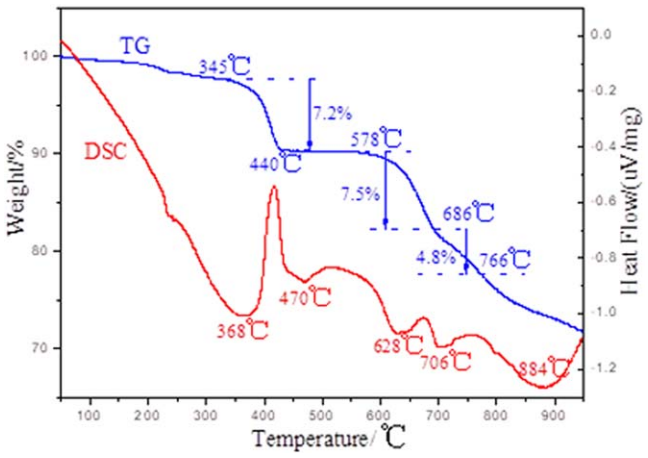


**Figure 2.** TG-DSC curves for jarosite waste.

of thermal decomposition was chosen at 450, 650, 700 and 750 °C. Figure 3 shows the XRD patterns of the raw material and the results of the decomposed products corresponding to the temperature of thermal decomposition. At 450 °C, it can be seen from the figure that the products of $Na_2SO_4$ and $PbSO_4$ are found. The reactions may be written as follows:

$$Na_2Fe_6(SO_4)_4(OH)_{12} \rightarrow Na_2SO_4 + Fe_2(SO_4)_3 + 6H_2O + 2Fe_2O_3 \quad [2]$$

$$PbFe_6(SO_4)_4(OH)_{12} \rightarrow PbSO_4 + Fe_2(SO_4)_3 + 6H_2O + 2Fe_2O_3 \quad [3]$$

The study found that the jarosite was completely dehydrated by 450 °C.[22] Thus, mass loss observed at 345 °C–440 °C is due to the evolved water vapour in the jarosite. The first endothermic peak is solid-solid phase transition in which Pb-jarosite and Na-jarosite are

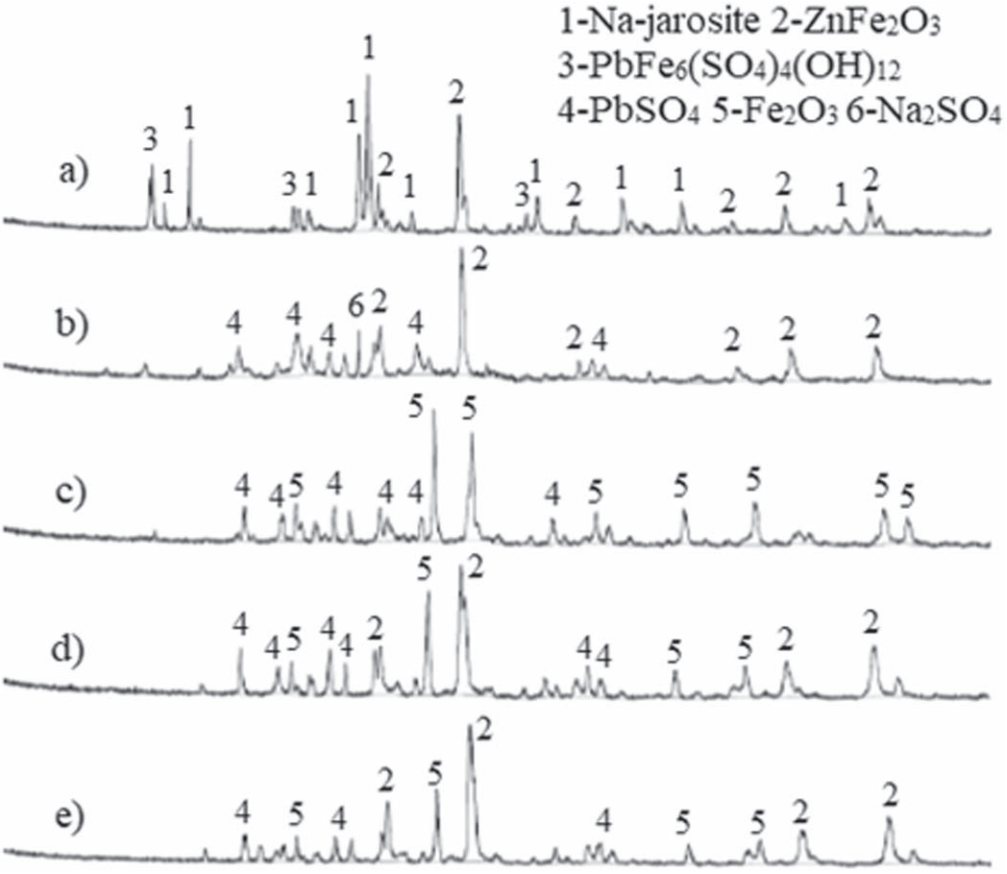


**Figure 3.** X-ray diffraction pattern of jarosite waste decomposition as a function of temperature.(a) Jarosite, (b) 450 ℃, (c) 650 ℃, (d) 700 ℃, (e) 750 ℃

decomposed and transformed into $Na_2SO_4$ and $PbSO_4$. Then, $Fe_2(SO_4)_3$ is further reacting with the loss of water and sulphur trioxide when the temperature is above 550 °C. The reaction is as follows:

$$Fe_2(SO_4)_3 \rightarrow Fe_2O_3 + 3SO_3 \quad [4]$$

Since the second endothermic peak is 670 °C, two temperatures, 650 and 700 °C, are chosen respectively in order to compare the difference of the product. At 650 °C, it is found that the morphology of the product is mainly lead sulfate and hematite. That may be because zinc ferrite reacts with ferric sulfate to produce zinc sulfate and hematite. The reaction may be summarized:

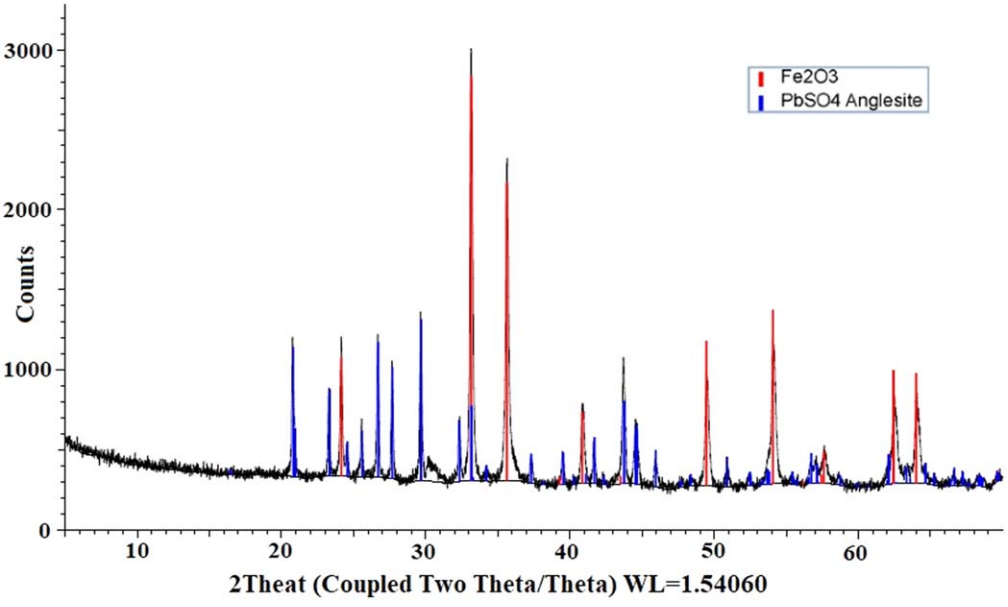


**Figure 4.** X-ray diffraction pattern of the product washed by water.

$$ZnFe_2O_4 + Fe_2(SO_4)_3 \rightarrow ZnSO_4 + 2Fe_2O_3 + 2SO_3 \quad [5]$$

The figure shows that the phase transition is almost completed when the temperature is close to 670 °C. The mass loss is mainly due to release of sulfur trioxide. However, at 700 °C, zinc ferrite is observed again, which shows that zinc sulfate may react with hematite to produce zinc ferrite and continuously release sulfur trioxide. The reaction may be written as follows:

$$ZnSO_4 + Fe_2O_3 \rightarrow ZnFe_2O_4 + SO_3 \quad [6]$$

The result obtained at 750 °C is similar to that at 700 °C. From the thermal analysis of jarosite waste, it shows that zinc ferrite can be formed by increasing the temperature. In order to avoid the formation of zinc ferrite, the temperature should be kept below 670 °C. Finally, in this study, the temperature of thermal decomposition is determined at 650 °C. Jarosite waste is heated to this temperature so as to produce hematite and lead sulfate.

***Two-step wash processing.***—The product was washed by two-step processing after thermal decomposition. The first step is to remove soluble matter by water, for instance, zinc sulfate. The XRD patterns of the product after washing by water is given in Fig. 4. It can be seen that soluble matter has been dissolved in water. There are hematite and lead sulfate left in the product of water washing. In order to make hematite more concentrated, sodium chloride solution is used to remove lead sulfate in the second step. Figure 5 shows that there is no presence of lead sulfate in the product washed by sodium chloride solution. That is because lead sulfate can dissolve in sodium chloride solution to form salt chloride complex to separate from hematite. In addition, the concentration of sodium chloride solution needs to be higher than 4 mol $l^{-1}$, which is beneficial for lead sulfate removal.

Hematite has been further concentrated through using the above process to obtain the raw material for electrolysis in the next step. Table II gives the composition of the main metallic elements in the products after the first and the second treatment processes compared with that of the raw material. It can be seen that the content of iron increases from 24.8% in jarosite to 49.9% in the product after the second treatment. Meanwhile, the contents of zinc and lead decrease from 8.6% and 4.9% to 4.5% and 0.9% respectively. In addition, the content of sulfur has been reduced to 0.4% after washing process. The element of sulfur in jarosite is present in combination with metals to form sulfate, for example zinc and lead sulfates. During the treatment processes, sulfur as sulfate radical dissolves in the solution to achieve the aim of sulfur removal.

Jarosite waste has been treated in order to be beneficial for electrolysis. In fact, if jarosite waste is directly used in electrolysis, it is difficult to obtain good results. The current efficiency of electrolysis will be low because there are many impurities in the raw material. Based on the above experiments, the results are promising for the aim of concentrating the iron content in jarosite waste.

***Cyclic voltammetry.***—As stated above, cyclic voltammetry studies were performed using a cavity electrode in aqueous NaOH electrolyte at 100 °C. The voltammogram is shown in Fig. 6 by using a cavity electrode filled with the particles from jarosite waste after treatment. The scan rate was 100 mV $s^{-1}$. Two scan potential ranges were used in the study. Towards the black curve of the cyclic voltammetry of unfilled $Fe_2O_3$, two peaks appear in a scan range of $-1.2 \sim 0.8$ V (vs reference electrode), where cathodic peak around $-1.1$ V and anodic peak nearly 0.5 V are the evolutions of $H_2$ and $O_2$ on Pt electrode respectively. Two cathodic peaks can be clearly seen after filled with $Fe_2O_3$ (blue curve). The first peak of the cathodic current around $-0.9$ V can be explained due to electrochemical reduction of $Fe_2O_3$, and the second peak is the reduction of $H^+$. Compared with platinum electrode, it was found that the evolution of hydrogen is at higher potential on Fe electrode. Compared to previous studies,[16,23,24] the results indicate that the reduction of hematite to metallic iron takes place in one step. The anodic peak between $-0.7$ V and $-0.4$ V might be corresponding to the oxidation of $Fe^{2+}$ to $Fe^{3+}$. The anodic peak at the positive potential 0.3 V is the oxidation of the steel rod used for the cavity electrode. For the red curve of the potential range $-1.0 - 0.5$ V, there is no oxidation peak of hydrogen gas and reduction peak of oxygen gas because the scan range of the potential is smaller.

***Electrolysis of suspension.***—Constant cell voltage electrolysis was carried out at 1.6 V for 4 h. The current decreases sharply at the beginning of electrolysis and stabilizes gradually with the extension of time. After electrolysis for 4 h, the product covered on the silver cathode is shown in Fig. 7. The black substance on the silver cathode was removed from the cathode, and then the sample analyzed by XRD and shown in Fig. 8. Although there are still hematite and lead compounds in the sample, metallic iron has been detected. The results indicate that it might be possible to reduce jarosite to iron during the electrolysis process.

This work would build upon attempts to develop a practical and economical process for recycling of jarosite waste. As matter of fact, many experiments have been done to reduce hematite to produce iron from alkaline suspensions of solid oxides, also including iron ore and iron-rich Bayer process residues. Compared to hematite,

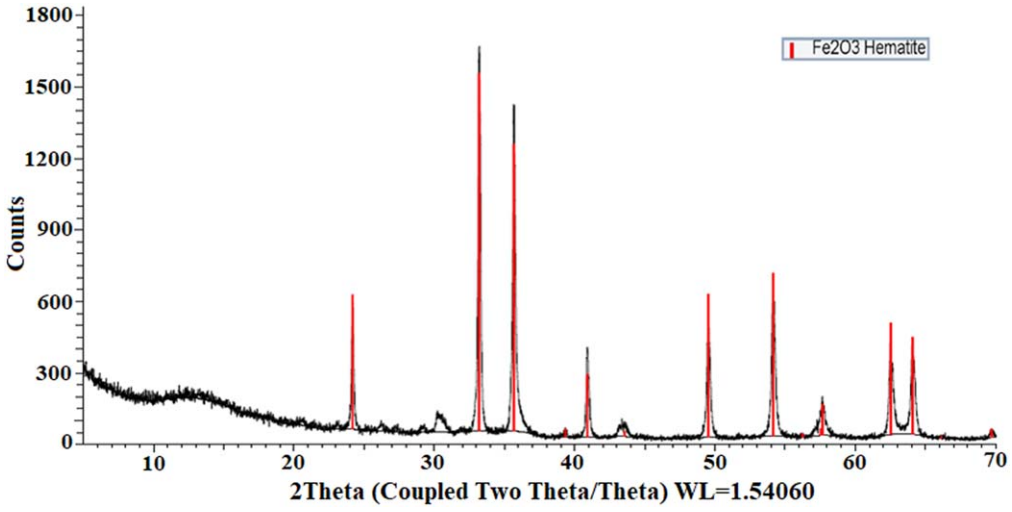


**Figure 5.** X-ray diffraction pattern of the product washed by sodium chloride solution.

**Table II. The composition of products analyzed by XRF.**

| Element | Content% | | |
|---|---|---|---|
| | Raw material | After 1st treatment | After 2nd treatment |
| Al | 1.2 | 2.4 | 2.7 |
| As | 0.18 | 0.5 | 0.6 |
| Ca | 1 | 0.6 | — |
| Cu | 0.54 | 0.3 | 0.2 |
| Fe | 24.8 | 42.3 | 49.9 |
| Mn | 0.55 | — | — |
| Pb | 4.9 | 10.0 | 0.9 |
| S | 12.5 | 2.0 | 0.4 |
| Sb | 0.08 | 0.2 | 0.1 |
| Si | 1.6 | — | 4.6 |
| Sn | 0.45 | 0.5 | 0.4 |
| Zn | 8.6 | 4.2 | 4.5 |

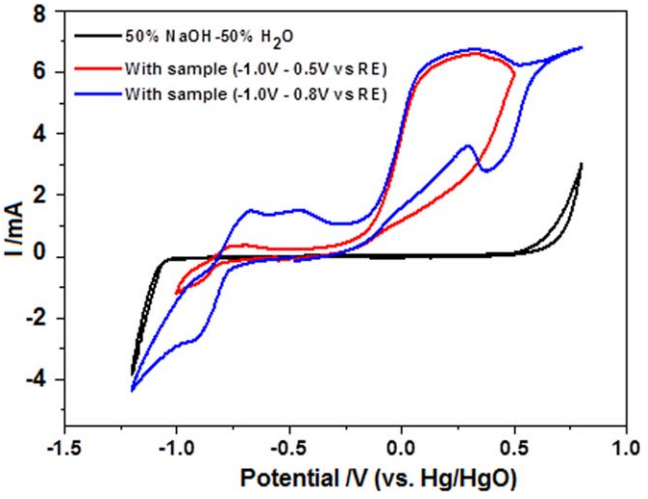


**Figure 6.** Cyclic voltammogram of the treated jarosite waste in a cavity electrode with a scan rate of 100 mV $s^{-1}$ at 100 °C.

there are some soluble and insoluble impurities in those iron-bearing raw materials and residues. The presence of impurities at the particle surface may affect the reactivity of the suspended particles at the cathode surface, so that hydrogen evolution occurs. Although the jarosite waste after washing has been reduced to iron during electrolysis, there are still some lead compounds in the product. Thus, the major aim is to optimize the pretreatment process to remove the impurities from jarosite waste as efficiently as possible. However, considerable efforts still need to be done in the future.

## Conclusions

In this work, thermal decomposition of the jarosite waste was carried out using TG-DSC under nitrogen atmosphere. There are three endothermic peaks during thermal analysis process, and the temperature of thermal decomposition is determined at 650 °C. The product after thermal decomposition was washed by two-step processing. The first step is to remove soluble matter by water. The second step is to remove lead sulfate by sodium chloride solution, where the concentration of the solution is higher than 4 mol $l^{-1}$. Cyclic voltammetry study for the residue after washing process was carried out using a cavity electrode at 100 °C in a 50 wt% NaOH aqueous solution. The reduction peaks were observed in the cathodic scan. Constant voltage electrolysis was performed by using electrolysis of suspension, where cell voltage was 1.6 V. Deposits after electrolysis were observed on the silver cathode and analyzed by XRD. The reduction reaction of iron oxide occurred at the surface of the cathode. The analysis results show that metallic iron was detected in the sample. Thus, through a series of pretreatment process, Jarosite waste can be used as the raw material of iron production by electrolysis.

## Acknowledgments

The financial support provided by the European Union H2020 SIDERWIN project is greatly appreciated.

## ORCID

Bo Qin https://orcid.org/0000-0002-9832-6206

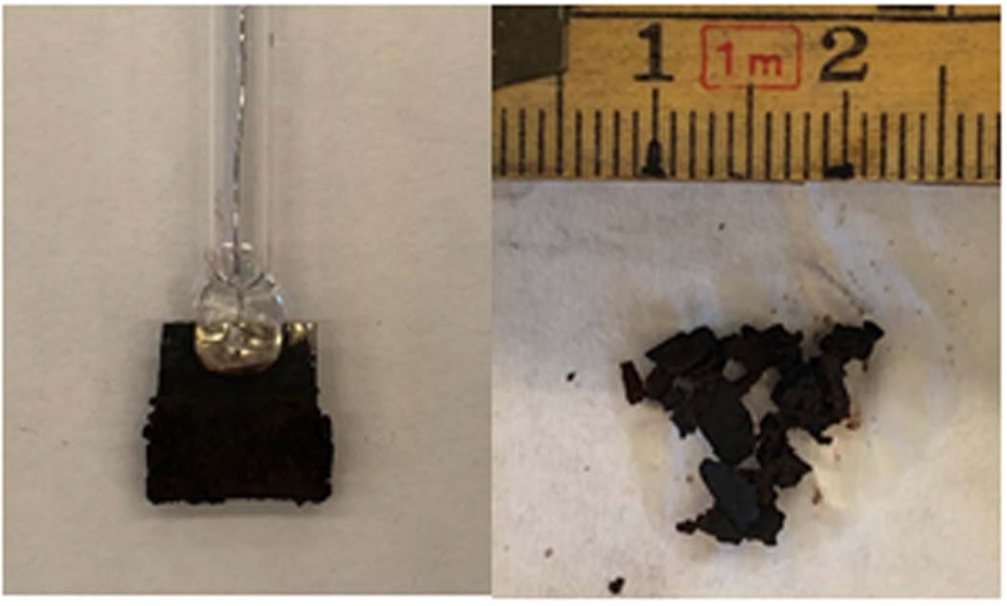


**Figure 7.** Picture of deposits from electrolysis.

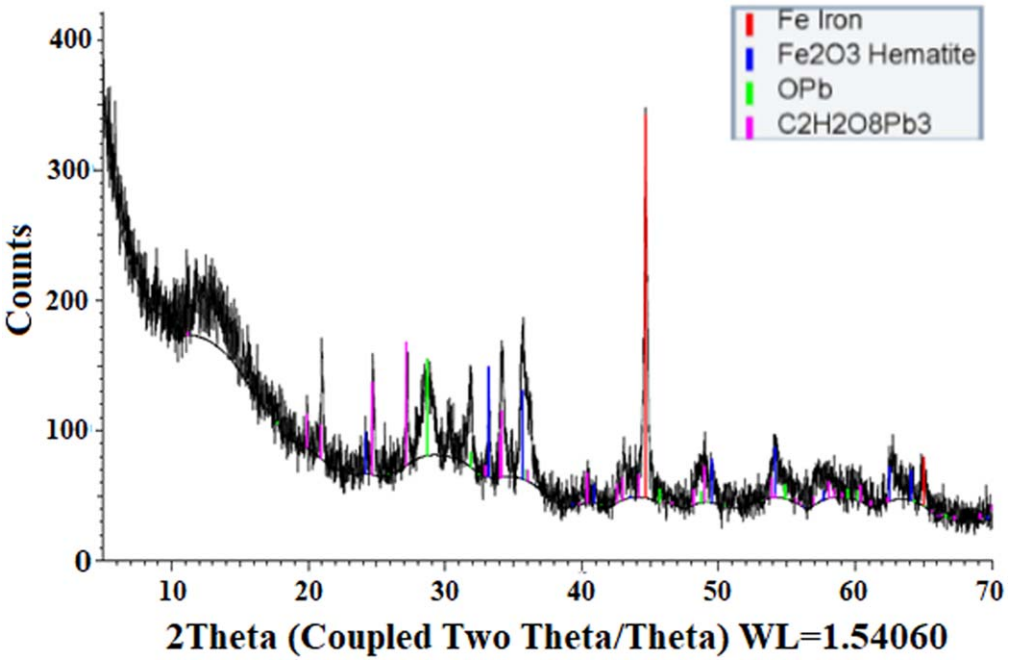


**Figure 8.** X-ray diffraction pattern of the deposit produced during electrolysis of 90 g $l^{-1}$ suspension particles.

## References


1. T. Buckby, S. Black, M. L. Coleman, and M. E. Hodson, *Mineral. Mag.*, **67**, 263 (2003).
2. G. K. Das, S. Anand, S. Acharya, and R. P. Das, *Hydrometallurgy.*, **38**, 263 (1995).
3. P. Asokan, M. Saxena, and S. R. Asolekar, *J. Hazard. Mater.*, **137**, 1589 (2006).
4. P. Asokan, M. Saxena, and S. R. Asolekar, *Sci. Total Environ.*, **359**, 232 (2006).
5. R. L. Frost, M. L. Weier, and W. Martens, *J. Therm. Anal. Calorim.*, **82**, 115 (2005).
6. D. Mombelli, C. Mapelli, S. Barella, A. Gruttadauria, and E. Spada, *J. Environ. Chem. Eng.*, **7**, 102966 (2019).
7. D. Q. Zhu, C. C. Yang, J. Pan, Z. Q. Guo, and S. W. Li, *J. Clean. Prod.*, **205**, 781 (2018).
8. E. N. Malenga, A. F. Maluba-Bafubiandi, and W. Nheta, *Hydrometallurgy.*, **155**, 69 (2015).
9. I. A. Reyes, F. Patino, M. U. Flores, T. Pandiyan, R. Cruz, E. J. Gutierrez, M. Reyes, and V. H. Flores, *Hydrometallurgy.*, **167**, 16 (2017).
10. S. Ju, Y. Zhang, Y. Zhang, P. Xue, and Y. Wang, *J. Hazard. Mater.*, **192**, 554 (2011).
11. M. Li, B. Peng, L. Chai, N. Peng, H. Yana, and D. Hou, *J. Hazard. Mater.*, **237–238**, 323 (2012).
12. Y. Wang, H. Yang, G. Zhang, J. Kang, and C. Wang, *Chem. Eng. J. Adv.*, **3**, 100023 (2020).
13. P. Mehra, R. C. Gupta, and B. S. Thomas, *J. Clean. Prod.*, **120**, 241 (2016).
14. V. A. Mymrin, H. A. Ponte, and P. R. Impinnisi, *Construct. Build. Mater.*, **19**, 141 (2005).
15. S. Ray, L. Daudi, H. Yadav, and G. D. Ransinchung, *J. Clean. Prod.*, **272**, 122546 (2020).
16. A. Allanore, H. Lavelaine, G. Valentin, J. P. Birat, and F. Lapicque, *J. Electrochem. Soc.*, **155**, E125.
17. B. Yuan, O. E. Kongstein, and G. M. Haarberg, *J. Electrochem. Soc.*, **156**, D64 (2009).
18. A. Maihatchi, M. N. Pons, Q. Ricoux, F. Goettmann, and F. Lapicque, *J. Electrochem. Sci. Eng.*, **10**, 95 (2020).
19. W. Kunda and H. Veltman, *Metall. Trans. B*, **10**, 439 (1979).
20. G. H. Qiu, M. Ma, D. Wang, X. Jin, X. Hu, and G. Z. Chen, *J. Electrochem. Soc.*, **152**, E328 (2005).
21. G. M. Haarberg and B. Khalaghi, *ECS Trans.*, **97**, 493 (2020).
22. J. L. Kulp and H. H. Adler, *Am. J. Sci.*, **248**, 475 (1950).
23. A. Allanore, H. Lavelaine, G. Valentin, J. P. Birat, P. Delcroix, and F. Lapicque, *Electrochim. Acta*, **55**, 4007 (2010).
24. M. Tokushige, O. E. Kongstein, and G. M. Haarberg, *ECS Trans.*, **50**, 103 (2013).